JOURNAL OF VIROLOGY, Jan. 1993, p. 131–141
0022-538X/93/010131-11$02.00/0

Vol. 67, No. 1

The Minor Capsid Protein VP1 of the Autonomous Parvovirus Minute Virus of Mice Is Dispensable for Encapsidation of Progeny Single-Stranded DNA but Is Required for Infectivity

GREGORY E. TULLIS, LISA R. BURGER, AND DAVID J. PINTEL*

Department of Molecular Microbiology and Immunology, School of Medicine, University of Missouri—Columbia, Columbia, Missouri 65212

Received 19 August 1992/Accepted 6 October 1992

The two capsid proteins of minute virus of mice, VP1 and VP2, are generated from a single large open reading frame by alternate splicing of the capsid gene mRNA. Examination of the replication of a series of mutants that express only VP1, only VP2, or neither capsid protein demonstrates that VP2 is necessary for the accumulation and encapsidation of virus progeny single-stranded DNA. VP1 is dispensable for these functions but is required to produce an infectious virion. Virus that lacks VP1 binds to cells as efficiently as wild-type minute virus of mice but fails to initiate a productive infection. Because neither capsid protein is required for viral-DNA replication, these results suggest that virus lacking VP1 is blocked at a step during virus entry, subsequent to cell binding and prior to the initiation of DNA replication.

Minute virus of mice (MVM) is a small, nonenveloped, T=1 icosahedral virus approximately 22 nm in diameter that packages a single negative-sense strand of DNA (15, 61). The viral capsid proteins VP1 and VP2 are translated from the viral R3 mRNAs generated from a promoter at map unit 38 (2, 31). The ratio of VP1 to VP2 found in both infected cells and assembled capsids depends on which splice donor site is used to excise the small intron common to all MVM transcripts (13, 29, 31, 42; see Fig. 1A). The major splicing pattern, first splice donor (D1; nucleotide [nt] 2280) to first acceptor (A1; nt 2377), which is used in approximately 70% of the molecules, deletes the initiating AUG for VP1, and translation of VP2 is initiated 690 nt further downstream at nt 2794. When the minor splicing pattern is used (D2 at nt 2317 to A2 at nt 2399 [25% of the R3 mRNA]), VP1 is initiated at nt 2286, 10 codons upstream of the splice donor, and is translated in the same open reading frame as VP2 after the splice junction. A third, rare splicing pattern (D1-A2 [not shown in Fig. 1A]), present in <5% of the viral RNA, has also been reported (42). R3 transcripts utilizing this splicing pattern should also produce VP2. A third capsid protein, VP3, is produced during infection by proteolytic cleavage of VP2, although it is not known whether this processing event is essential for virus infection (58, 59, 62).

The processing of VP2 in full MVM virions can be mimicked in vitro by digestion with trypsin, although the protease site in vivo is not identical to the trypsin-sensitive site (46, 59, 62). Empty MVM capsids are resistant to protease digestion both in vitro and in vivo (15, 46, 59), suggesting that the capsid undergoes a conformational change upon encapsidation of viral DNA which exposes the processing site in VP2. Although this same processing site is also found in VP1, along with 22 other potential trypsin sites in the N terminus, VP1 is resistant to proteolytic digestion in both empty capsids and full virions, even under conditions in which 80% of the VP2 molecules have been cleaved to VP3 (59). These results suggest that the N-terminal domain of VP1, which is unique to VP1, remains on the interior of the capsid; together with the observation that the N-terminal region of VP1 is fairly basic (10.6 mol% lysine and 6.3 mol% arginine), these results have led to the proposal that this region consists of a DNA-binding domain involved in the encapsidation and stabilization of the viral single-stranded DNA (ssDNA) within the protein coat (48, 59).

Mutational analysis of the capsid genes of MVM, H1, and adeno-associated virus (AAV) has demonstrated that the capsid proteins are required for the accumulation of progeny viral ssDNA (27, 37, 50, 60). Electron micrographs show capsid structures associated with the ends of both ssDNA and double-stranded DNA forms, suggesting that the viral ssDNA is packaged into intact preformed capsids (25). In addition, two types of defective genomes are packaged during an MVM infection: viral ssDNAs with internal deletions and a double-stranded DNA form containing the right end (or 5′ hairpin), suggesting that all of the *cis* signals required for packaging are found within the 5′ end (20). Together, these results suggest a model in which viral DNA is sequestered and packaged 5′ to 3′ by the binding of the capsid to the 5′ end of viral DNA as the opposite strand is being replicated.

Unlike capsid mutants which disrupt both VP1 and VP2, mutants in AAV that are now known to affect only VP1 produce progeny ssDNA but little or no infectious virus (27, 60). These results suggested either that VP1 is dispensable for the accumulation of ssDNA but necessary for its encapsidation or, alternatively, that VP1 is required to produce a competent or stable particle. Willwand and Hirt (65) have recently demonstrated that intact MVM empty capsids as well as gel-purified VP1, but not VP2, bind specifically to the left or 3′ hairpin of MVM DNA. These results might suggest that encapsidation of MVM viral DNA is dependent on VP1 and begins at the 3′ end of the viral ssDNA after replication of the complementary strand is completed but as such would be in contrast to the finding of packaged MVM-defective DNA containing only the 5′ end of viral DNA. Similar binding properties have also been reported for the VP1 of Aleutian disease virus (ADV) (66) and VP2 of bovine parvovirus (BPV) (32, 39). (BPV produces an additional, larger

* Corresponding author.

coat protein; therefore, VP2 of BPV may be equivalent to VP1 of MVM [11] [see Fig. 10].)

In this report, we examine the replication and infectivity of MVM mutants that express only VP1, only VP2, or neither capsid protein. Our results demonstrate that VP2 is both necessary and sufficient for the replication and encapsidation of viral ssDNA and that VP1 is dispensable for these functions. However, VP1 is required to produce an infectious particle. Virus that lacks VP1 bound to the surface of cells as well as or better than wild-type MVM (*wt*) but failed to initiate a productive infection. Because VP1 mutants replicate in a manner similar to that of *wt* following DNA transfection, they appear to be blocked subsequent to cell binding and prior to the initiation of DNA replication. We suggest that VP1 may be required for transport of the incoming particle or viral DNA strand to the nucleus and that this pathway may be distinct from the transport of de novo-synthesized proteins or assembled empty capsids to the nucleus because VP2, by itself, is localized to the nucleus and packages viral DNA.

MATERIALS AND METHODS

Construction of the mutants and viral isolation. pMVM(D1-A1) and pMVM(D2-A2) were constructed by replacing the *Xho*I-to-*Hin*dIII fragment (nt 2071 to 2651) of the infectious clone, pMVM (37, 38, 63), with the analogous fragment from cDNA clones that had the small intron either from nt 2280 (D1) to 2377 (A1) or from nt 2317 (D2) to 2399 (A2) excised (13). A frameshift was introduced in the VP1 open reading frame by linearizing pMVM with *Bss*HII (nt 2635), digesting with mung bean nuclease (New England Biolabs, Beverly, Mass.), and religating to yield pMVM(VP1*2635*). Similarly, a frameshift at the *Bgl*II site (nt 3451), which disrupts both VP1 and VP2, was constructed by linearizing pMVM with *Bgl*II and filling in the restriction site with the Klenow fragment of DNA polymerase (Promega Biotec, Madison, Wis.) to generate pMVM(VP1/*23451*). All constructs were propagated in *Escherichia coli* JC8111 and monitored by restriction enzyme digestion to ensure the integrity of the right-end palindrome (7). Capsid proteins from all four of these mutants were immunoprecipitated as previously described (31) following DNA transfection of Cos1 (23), NB324K (57), and murine $A9_{2L}$ (34) cells by the calcium phosphate precipitation method (31). As expected (13), only VP2 was detected in pMVM(D1-A1)- and pMVM (VP1*2635*)-transfected cells and only VP1 was detected with pMVM(D2-A2) (data not shown).

MVM(D1-A1) was obtained by transfecting Cos1 cells (4×10^5 cells per 60-mm plate) with 5 μg of DNA, and virus was released from the cells in TE 8.7 (10 mM Tris-HCl [pH 8.7], 1 mM EDTA) 48 h after transfection, as previously described (57). Full virions were isolated by centrifugation ($250,000 \times g$) for 3.5 h through a 10 to 40% sucrose gradient in TE (pH 8.0) in an SW41 rotor (Beckman Instruments, Palo Alto, Calif.). Fractions containing full virions were identified by Southern blot analysis (54) for viral ssDNA. Peak fractions were pooled and viral particles were concentrated by centrifugation ($250,000 \times g$) in an SW50.1 rotor (Beckman Instruments) for 6 h and resuspended in TE 8.7. Full MVM(VP1*2635*) virions were isolated in the same way from DMN4A cells, a chemically transformed derivative of BHK cells (8), 24 h after transfection with pMVM(VP1*2635*).

Cell binding, virus infectivity, and export of progeny virions. Assays for cell binding, virus infectivity, and export of progeny virions have been described in detail elsewhere (62). $A9_{2L}$ cells were prelabeled for 24 h with [^{3}H]thymidine (1 μCi/ml) prior to seeding (4×10^5 cells per 60-mm plate), so that the amount of virus bound could be standardized relative to an equivalent number of cells.

For binding assays, monolayers of ^{3}H-labeled $A9_{2L}$ cells were overlaid for 10, 20, or 30 min at 37°C with MVM (VP1*2635*) or *wt* sucrose gradient-purified virions (in 0.2 ml) that had been equilibrated for ssDNA content in the presence of aphidicolin (12 μg/ml) to prevent the conversion of the input ssDNA to double-stranded DNA (15). For *wt*, the amount of input virus corresponded to approximately 0.01 infectious units per cell, as measured by in situ plaque assay (see Fig. 5) (10, 67). At 10, 20, and 30 min after infection, the cells were washed four times with cold phosphate-buffered saline (PBS), pelleted, and stored frozen at −70°C until all samples had been collected. Cells were lysed in lysis buffer (2% sodium dodecyl sulfate [SDS], 0.15 M NaCl, 10 mM Tris [pH 8.0], 1 mM EDTA, 0.25 mg of proteinase K per ml) at 37°C for 30 min and incubated at 65°C for another 30 min or until the cell pellet was completely lysed. Cellular DNA was sheared by passing the samples through a 25-gauge needle. Aliquots (2 μl) of each sample were applied to DE81 filters in quadruplicate, and incorporated ^{3}H was assayed as described elsewhere (35). Equivalent amounts of ^{3}H-labeled samples were subjected to agarose gel electrophoresis (1% agarose), and the amounts of cellular DNA present were confirmed by scanning a photographic negative (Polaroid type 55 film) of the ethidium bromide (5 μg/ml)-stained gel with a laser densitometer (LKB, Bromma, Sweden) (43). The amount of viral DNA present in each sample was detected by Southern blotting and quantified with a Molecular Dynamics Phosphorimager.

To examine DNA replication of MVM(VP1*2635*) by viral infection, ^{3}H-labeled $A9_{2L}$ cells were infected with equivalent amounts of *wt* and MVM(VP1*2635*) sucrose gradient-purified virions for 30 min at 37°C as described above. Cells were refed with Dulbecco modified Eagle medium containing 5% fetal calf serum and neuraminidase (0.05 U/ml; Sigma Chemical Company, St. Louis, Mo.) to prevent reinfection. At various times after infection, the cells were harvested and lysed as described above, and virus replicative forms (RF) were detected by Southern blotting.

To examine the efficiency of export of progeny virus to the medium, $A9_{2L}$ cells were transfected with either pMVM or pMVM(VP1*2635*) (5 μg per plate) and neuraminidase (0.3 U/ml) was added to the medium. Because of the unusually long time course of this experiment, additional neuraminidase (0.2 U/ml) was added 48 h after transfection. At 48, 72, and 96 h after transfection, the cells were either scraped into the medium and the total sample was lysed as described above by the addition of SDS to a final concentration of 2% (total) or the cells were isolated from the medium by centrifugation, rinsed with an isotonic borate buffer (pH 9.0) to remove any virus that might have been bound to the surface of the cells, and lysed separately in PBS containing 2% SDS (cells). Aliquots of the cleared medium before and after the addition of the borate rinses were adjusted to 2% SDS as described above. All samples were treated with proteinase K (0.25 mg/ml) for 1 h at 37°C prior to agarose gel electrophoresis. The amount of cellular DNA present in each sample was quantified as described above. Viral DNA was detected by Southern blotting and quantified with a Phosphorimager. The amount of cell-associated progeny virus was calculated by comparing the amount of ssDNA present in the isolated cells with the amount present in the total sample (cells plus medium).

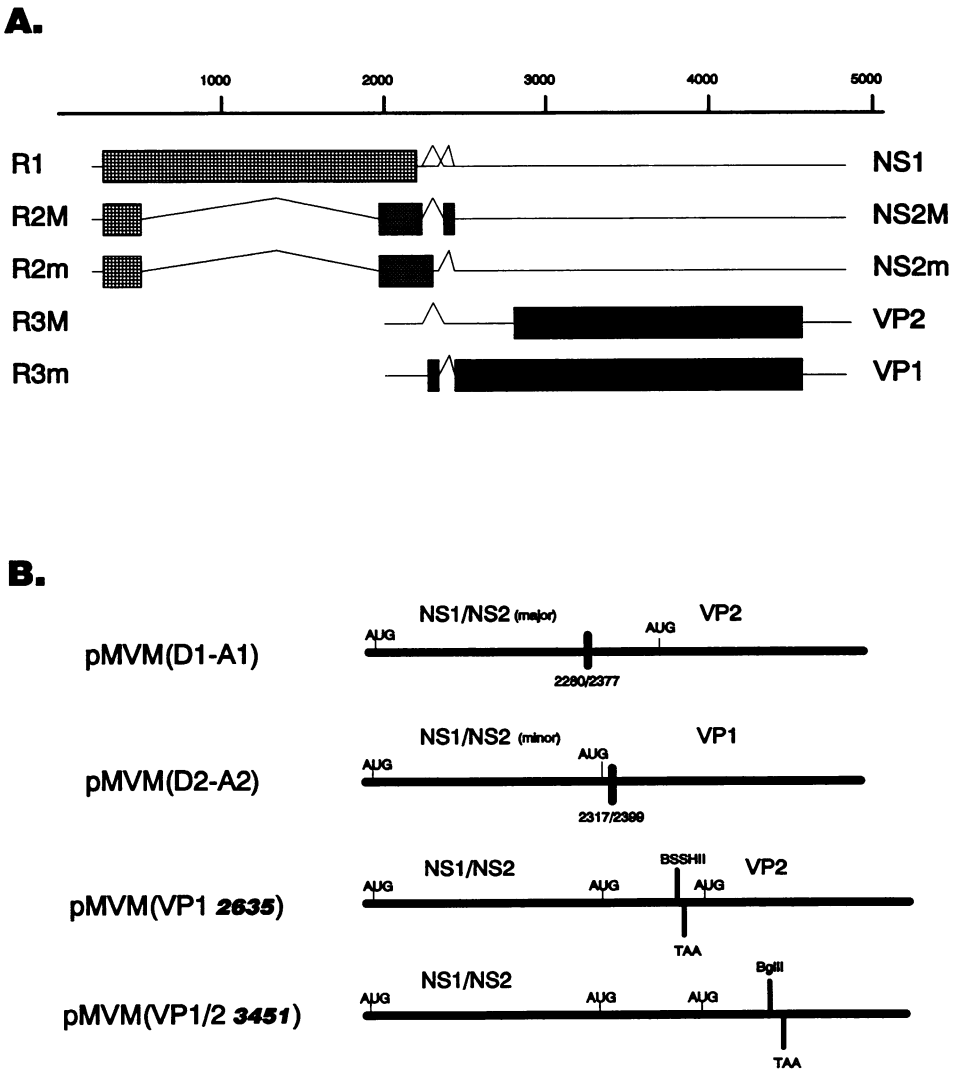

FIG. 1. (A) Transcription map and genetic organization of MVM. MVM mRNAs are listed on the left, and their respective gene products are listed on the right. RNAs are designated M (major) or m (minor) depending on whether the major (D1-A1) or minor (D2-A2) splicing pattern is used to excise the small intron common to all of the mRNA classes. A third, rare splicing pattern (D1-A2) has also been reported but is not shown. Scale at the top is in nucleotides. (B) Diagram of the coding regions of the mutants used in this study. Proteins produced by these mutants are indicated above the horizontal line. Vertical lines represent sites of alteration. Initiating AUG codons for the nonstructural proteins as well as VP1 and VP2 are also indicated.

RESULTS

To distinguish the relative contributions of the virus capsid proteins VP1 and VP2 during virus replication, we have constructed a series of mutants in the infectious clone of MVM that, in addition to the viral nonstructural proteins, express only VP1, only VP2, or neither capsid protein (Fig. 1B). Mutants pMVM(D1-A1) and pMVM(D2-A2) were reconstructed from cDNA clones across the small-splice region (13). Thus, pMVM(D1-A1), which expresses VP2, is a full-length infectious clone of MVM, except that the sequences between D1 (nt 2280) and A1 (nt 2377) have been deleted. Likewise, pMVM(D2-A2), which expresses only VP1, is a full-length clone of MVM except that nt 2317 (D2) has been joined to nt 2399 (A2). Because the choice of small-splice donor and acceptor also affects the 25-kDa nonstructural protein, NS2 (Fig. 1A), pMVM(D1-A1) expresses only the major isoform of NS2 and pMVM(D2-A2) expresses only the minor form. These two forms of NS2 vary only in their last six amino acids (aa). Mutant pMVM(VP1*2635*) has a frameshift at the *Bss*HII site at nt 2635 that prematurely terminates VP1 shortly after this mutation but leaves VP2 and the nonstructural proteins unaltered (Fig. 1). Similarly, another frameshift mutant, pMVM(VP1/*23451*), truncates both VP1 and VP2 with no effect on the nonstructural proteins.

VP2 is necessary and sufficient to produce progeny viral DNA. Following DNA transfection into murine $A9_{2L}$ fibroblasts, all four of these mutants accumulated approximately 10-fold fewer double-stranded, monomer, and dimer RF DNAs than *wt* pMVM (Fig. 2A). This difference in RF accumulation is due to a failure of these mutants to spread from the originally transfected cell rather than a deficiency in

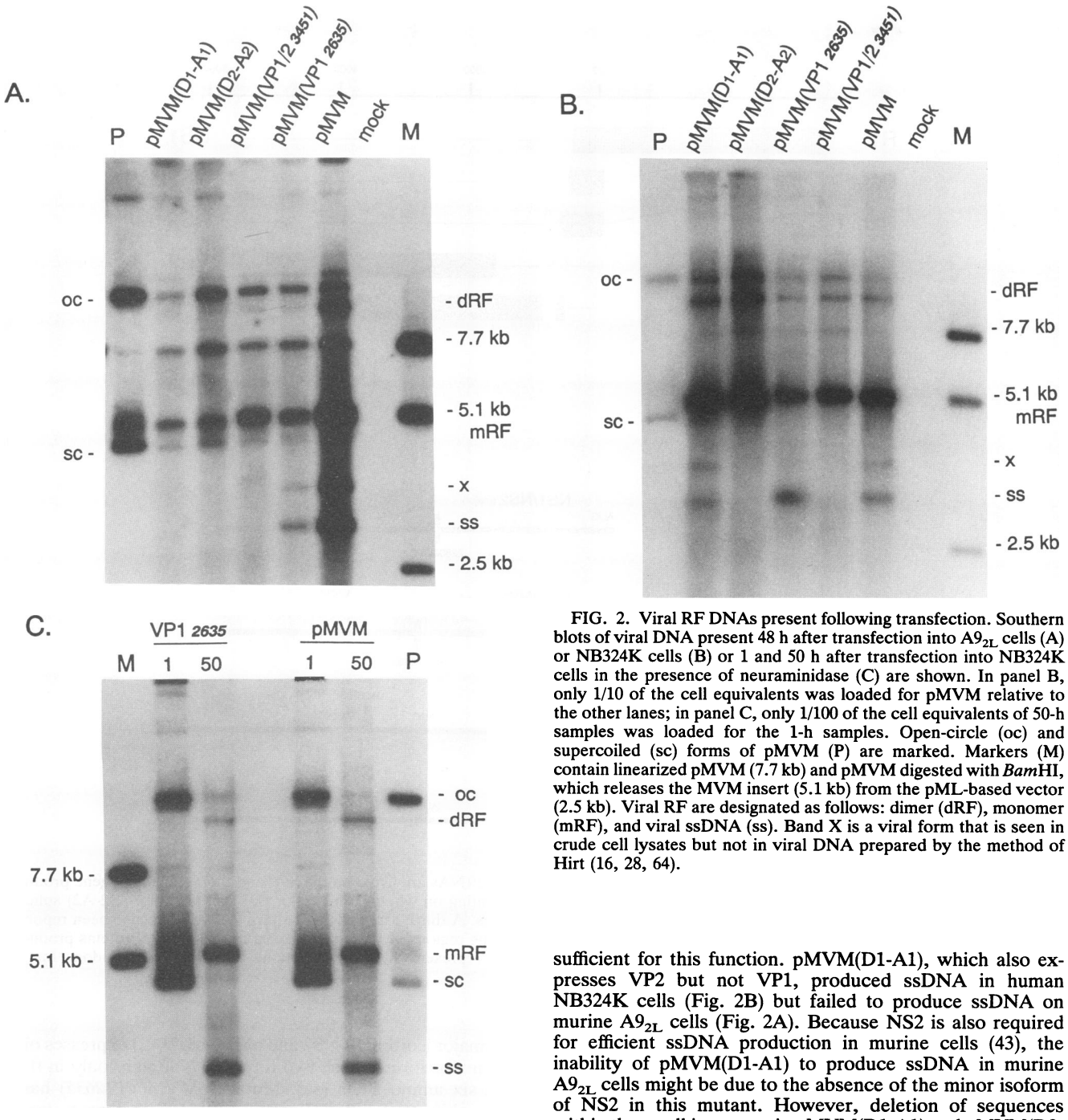

FIG. 2. Viral RF DNAs present following transfection. Southern blots of viral DNA present 48 h after transfection into $A9_{2L}$ cells (A) or NB324K cells (B) or 1 and 50 h after transfection into NB324K cells in the presence of neuraminidase (C) are shown. In panel B, only 1/10 of the cell equivalents was loaded for pMVM relative to the other lanes; in panel C, only 1/100 of the cell equivalents of 50-h samples was loaded for the 1-h samples. Open-circle (oc) and supercoiled (sc) forms of pMVM (P) are marked. Markers (M) contain linearized pMVM (7.7 kb) and pMVM digested with *Bam*HI, which releases the MVM insert (5.1 kb) from the pML-based vector (2.5 kb). Viral RF are designated as follows: dimer (dRF), monomer (mRF), and viral ssDNA (ss). Band X is a viral form that is seen in crude cell lysates but not in viral DNA prepared by the method of Hirt (16, 28, 64).

DNA replication, because all of the mutants accumulated levels of RF similar to *wt* levels when neuraminidase, which presumably inhibits MVM binding by cleaving sialic acid residues on the cell surface, was added to the medium to prevent reinfection (data not shown).

As expected, pMVM(VP1/*23451*), which produces neither VP1 nor VP2, failed to accumulate progeny ssDNA in both $A9_{2L}$ and NB324K cells (Fig. 2A and B). pMVM(VP1*2635*), which prematurely truncates VP1, leaving VP2 unaltered, was able to efficiently produce progeny ssDNA in both cell lines, demonstrating that the major capsid protein VP2 is sufficient for this function. pMVM(D1-A1), which also expresses VP2 but not VP1, produced ssDNA in human NB324K cells (Fig. 2B) but failed to produce ssDNA on murine $A9_{2L}$ cells (Fig. 2A). Because NS2 is also required for efficient ssDNA production in murine cells (43), the inability of pMVM(D1-A1) to produce ssDNA in murine $A9_{2L}$ cells might be due to the absence of the minor isoform of NS2 in this mutant. However, deletion of sequences within the small intron, as in pMVM(D1-A1) and pMVM(D2-A2), also inhibits the accumulation of the NS2 mRNA (R2) resulting in the overexpression of R1, which encodes the large nonstructural protein NS1 (53). Therefore, the underexpression of NS2 or overexpression of NS1 may also contribute to this phenotype. pMVM(D2-A2), on the other hand, failed to produce ssDNA following transfection of $A9_{2L}$ (Fig. 2A), NB324K (Fig. 2B), or Cos1 cells (data not shown). Because NS2 mutants are only two- to threefold deficient in progeny ssDNA accumulation following transfection of NB324K cells (43, 44) and because overexpression of NS1 does not inhibit ssDNA accumulation in pMVM(D1-A1)-transfected NB324K cells, these results suggest that

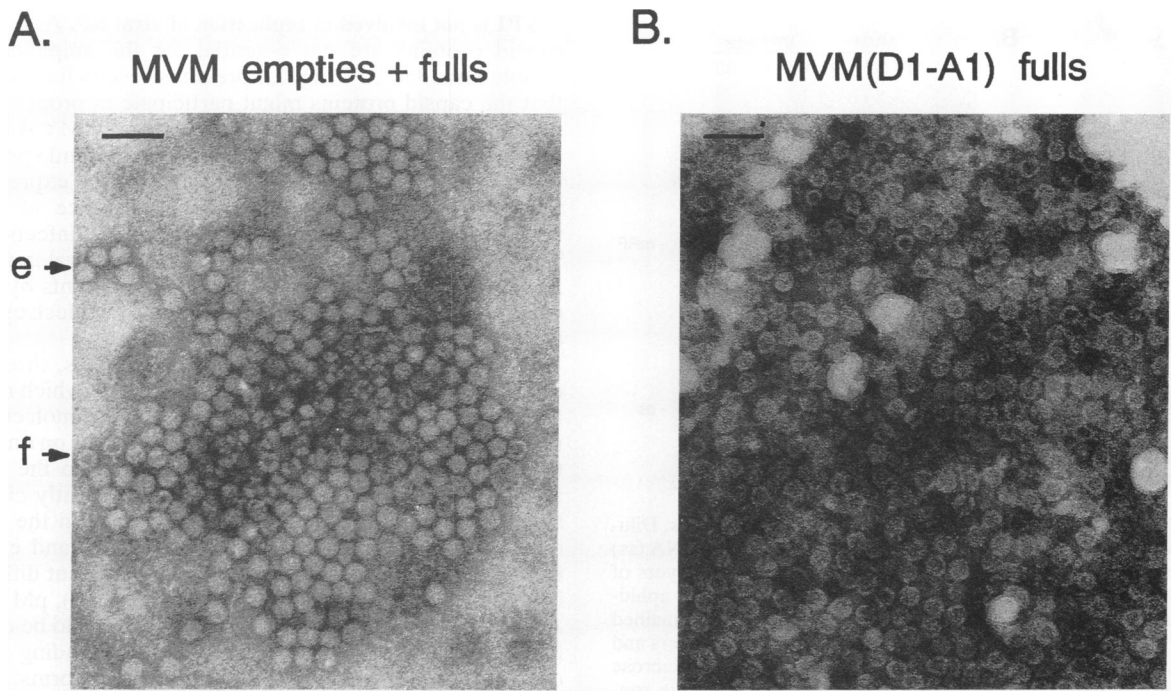

FIG. 3. Electron micrographs of *wt* in TE 8.7 (A) and sucrose gradient-purified full MVM(D1-A1) virions produced in Cos1 cells resuspended in TE 8.7 (B). Both samples were prepared with 3% phosphotungstic acid (instrument magnification, ×80,000). The bar represents 100 nm. e, empty virion; f, full virion.

VP1, unlike VP2, is not sufficient to produce progeny ssDNA.

In several experiments, it appeared that pMVM(VP1*2635*) produced a greater amount of ssDNA per monomer RF (mRF) than *wt* pMVM (Fig. 2B). However, during a normal MVM infection, the ratio of progeny ssDNA to mRF can increase dramatically late in an infection, and the kinetics of MVM replication following DNA transfection depends on the efficiency of the transfection (15, 37, 61a). In an experiment in which the amount of plasmid initially transfected into the cells was approximately equivalent, pMVM (VP1*2635*) and pMVM produced similar amounts of ssDNA relative to mRF (Fig. 2C).

VP2 is sufficient to assemble into a capsid structure and package viral DNA. During MVM infection, all of the ssDNA produced is normally encapsidated (15). Therefore, because pMVM(VP1*2635*) and pMVM(D1-A1) accumulated ssDNA following transfection into NB324K cells (Fig. 2B), it seemed likely that this ssDNA was packaged, even though these mutants were unable to produce plaques on these cells (data not shown). Virus particles could be isolated from sucrose gradients of lysates of Cos1 and DMN4A cells transfected with pMVM, pMVM(D1-A1), and pMVM (VP1*2635*). ssDNA from both pMVM(D1-A1) and pMVM (VP1*2635*) was detected by Southern blot analysis in a position in the gradient similar to that of *wt* full virions, suggesting that this DNA was indeed encapsidated; however, no full virions from pMVM(D2-A2)-transfected cells were detected by Southern blot analysis (data not shown). Sucrose gradient fractions that contained full virions from Cos1 cells transfected with either *wt* or pMVM(D1-A1) were pooled, and the virus particles were concentrated by centrifugation. The presence of full MVM(D1-A1) particles, which are morphologically indistinguishable from *wt* full virions, was confirmed by electron microscopy (Fig. 3).

VP1 is required to produce an infectious virion. Although pMVM(VP1*2635*) replicated and produced progeny virus following transfection into either $A9_{2L}$ or NB324K cells, it did not produce plaques on either cell line (data not shown). MVM(VP1*2635*) must, therefore, be blocked in egress from the initially transfected cell, in initiating an infection, or both. To characterize the infectivity of virus that contains only VP2, we first tested the ability of MVM(VP1*2635*) to bind to target cells. Monolayers of $A9_{2L}$ cells were overlaid for various times with sucrose gradient-purified *wt* or MVM(VP1*2635*) full virions, normalized for their ssDNA contents. After extensive washing, the amount of MVM (VP1*2635*) that remained bound to the cells, as determined by Southern blot analysis, was equal to or greater than the amount of *wt* (Fig. 4).

Since MVM(VP1*2635*) was not defective in this simple cell-binding assay, we next looked at the ability of this mutant to initiate DNA replication. Equivalent amounts of sucrose gradient-purified *wt* and MVM(VP1*2635*) full virions, as assayed by their DNA contents, were used to infect $A9_{2L}$ cells, and the amounts of subsequent viral replicative DNA present were determined by Southern blot analysis. Although similar amounts of input *wt* and MVM(VP1*2635*) virions had bound to the cells after 30 min, MVM(VP1*2635*) produced no double-stranded DNA forms by 24 h postinfection, suggesting that this mutant is blocked at some step subsequent to binding to cells and prior to the initiation of DNA replication (Fig. 5A). We have also examined the ability of MVM(VP1*2635*) to initiate a productive infection by an in situ plaque assay (10, 67) with monolayers of $A9_{2L}$ cells infected with equivalent amounts of *wt* and

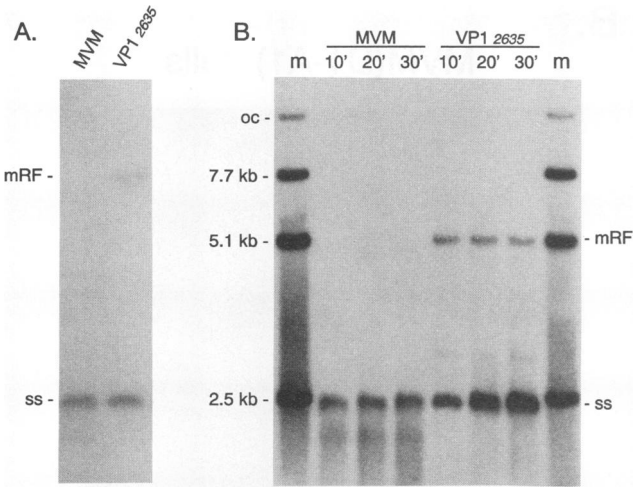

FIG. 4. Binding of MVM and MVM(VP1*2635*) to $A9_{2L}$ cells. Dilutions of MVM and MVM(VP1*2635*) were equilibrated for ssDNA (ss) content by Southern blotting (A) and then applied to monolayers of $A9_{2L}$ cells for 10, 20, and 30 min at 37°C in the presence of aphidicolin. After extensive rinsing, the amount of virus that remained bound to the cells was assayed by Southern blotting (B). Markers and viral RF are designated as described in the legend to Fig. 2. Sucrose gradient-isolated stocks of MVM(VP1*2635*), but not *wt*, have routinely contained significant amounts of mRF (A); however, the significance of this observation is not known at this time. oc, open-circle forms.

MVM(VP1*2635*), as determined by DNA content (Fig. 5B). No infectious centers were detected with MVM(VP1*2635*)-infected cells, even at the lowest dilution. Therefore, MVM(VP1*2635*) was defective by at least 4 orders of magnitude in the initiation of a productive viral infection compared with *wt* (Fig. 5C).

VP1 is not required for the efficient export of progeny virions from the cell. Most of the progeny ssDNA present during an MVM infection of highly synchronized $A9_{2L}$ cells is found in the medium as early as 6 h postinfection, suggesting that progeny virions are exported out of the cell soon after they are assembled and well before cytolysis occurs (17). A similar effect in the infection of asynchronous cells can be observed if neuraminidase is added to the medium to prevent binding of virus to the cell surface (62). To determine whether viral particles lacking VP1 could be efficiently transported out of the cell, we examined the localization of viral ssDNA following transfection of $A9_{2L}$ cells with either pMVM or pMVM(VP1*2635*). At various times after transfection, the cells were scraped into the medium and either the entire sample was lysed with 2% SDS (total) or, alternatively, the cells were isolated from the medium by low-speed centrifugation and resuspended in PBS plus 2% SDS (cells). The amount of viral DNA in each sample was determined by Southern blot analysis after it was ensured that an approximately equal number of cell equivalents, on the basis of cellular DNA contents, had been loaded in each lane. An approximately equal fraction of the cell-free supernatant was also loaded on the gel. In the presence of neuraminidase, less than 20% of the progeny ssDNA produced by either MVM or MVM(VP1*2635*) was associated with the cells at 96 h after transfection, indicating that VP1 is not required for this process (Fig. 6). Similar results were also observed at 48 and 72 h after transfection (data not shown).

VP1 is not involved in replication of viral RF. Although the capsid proteins are not essential for the amplification of double-stranded RF (Fig. 2), previous results had suggested that the capsid proteins might participate in proper maturation of the viral left-hand (3′) end: (i) empty MVM capsids, as well as reconstituted VP1 (but not VP2), bind specifically to the 3′ end of MVM DNA (65), and (ii) the expression of the capsid proteins precedes the appearance of left-end turnaround forms in a highly synchronized infection (64). Therefore, we chose to examine specific viral replicative intermediates generated by these capsid mutants by using a combination of two-dimensional agarose gel electrophoresis and restriction enzyme analysis.

By two-dimensional agarose electrophoresis, three forms of mRF can be identified: the extended form, which migrates as a typical, 5-kb, double-stranded DNA molecule; the turnaround forms, which are covalently closed on one end of the molecule and migrate as 10-kb strands in the second, alkaline dimension; and a form that is covalently closed on both ends and migrates as an ssDNA circle in the alkaline dimension (14; Fig. 7A). Similar turnaround and extended forms of dimer RF are also found. No significant differences in any major RF generated by pMVM (Fig. 7B), pMVM(D1-A1) (Fig. 7D), or pMVM(D2-A2) (Fig. 7C) could be detected following transfection of NB324K cells, including the percentages of total turnaround and extended forms. pMVM (D1-A1) did produce less ssDNA per mRF than pMVM in this experiment (compare Fig. 7B and D); however, this is likely to be an effect of NS2 rather than VP1 because (i) pMVM(VP1*2635*) did not show this effect (Fig. 2; data not shown) and (ii) NS2 mutants exhibit a reduction in ssDNA accumulation in these cells (44). Interestingly, these assays also expose a small amount of ssDNA produced by pMVM (D2-A2); however, it is less than 1/100 of the amount found in *wt*-transfected cells (compare Fig. 7B and C).

Although two-dimensional agarose gel electrophoresis can distinguish turnaround from extended forms of MVM DNA, this analysis cannot determine whether these turnaround forms are covalently closed on the left or right end of the molecule. The ratio of turnaround to extended forms on the left and right ends of RF can be determined directly by restriction enzyme analysis. By this analysis, all of the capsid mutants accumulated similar amounts of turnaround forms as *wt* in both the left and right ends of replicative DNA (Fig. 8). Thus, our results suggest that VP1 is not required for the correct maturation of the 3′ end of virus-replicative intermediates.

DISCUSSION

Our analysis of two MVM mutants that express only VP2 and not VP1 indicates that VP2 is both required and sufficient to assemble into capsids and package viral ssDNA. However, VP1 is required to produce an infectious virus. Virions lacking VP1 bound cells as well as or better than *wt* but failed to initiate a productive infection. Because mutants that lack VP1 replicate to *wt* levels following transfection into NB324K cells, it appears that these mutants are blocked at some step subsequent to cell binding but prior to the initiation of viral-DNA replication, such as virus uptake or transport to the nucleus.

VP1 has previously been proposed to be involved in the encapsidation and stabilization of viral ssDNA in the protein coat because the N-terminal region of VP1 is fairly basic and is presumably found on the interior of the capsid (48, 59). The finding that VP1, but not VP2, bound specifically to the

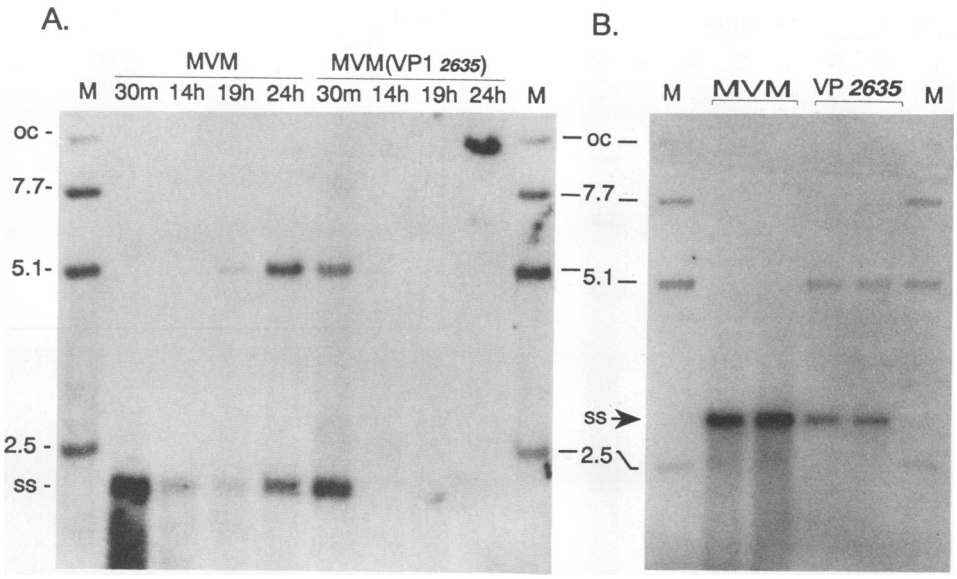

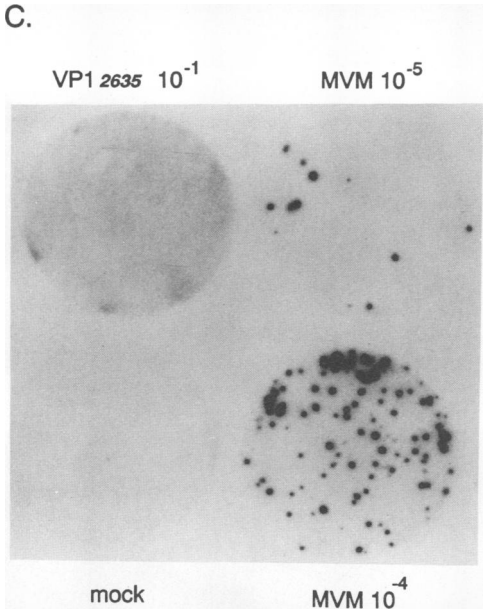

FIG. 5. Infectivities of MVM and MVM(VP1*2635*) virions. (A) Southern blot of viral RF present at 0.5, 14, 19, and 24 h after infection of asynchronous $A9_{2L}$ cells; (B) viral DNA present in 10^{-1} dilutions of MVM and MVM(VP1*2635*) used in the infectious-center assay shown in panel C. These vary by twofold as determined by Phosphorimager analysis. (C) Monolayers of $A9_{2L}$ cells infected with 0.2 ml of various dilutions of either MVM or MVM(VP1*2635*) were transferred to nitrocellulose and hybridized to a ^{32}P-labeled, MVM-specific probe prepared with random primers (Pharmacia, Piscataway, N.J.). Only one of the duplicate filters for each dilution is shown. ss, ssDNA; oc, open-circular forms; M, markers.

left or 3′ hairpin of MVM DNA further suggested that VP1 plays a role in the replication or encapsidation of viral DNA (65), although this binding occurred on the opposite end of the DNA predicted to contain the necessary packaging signals, on the basis of the characterization of defective interfering particles (20). Previous genetic analysis of AAV demonstrated that viral ssDNA could be produced in the absence of VP1; however, these studies did not directly address whether this DNA was encapsidated. Our results clearly demonstrate that VP1 is not required for the encapsidation of ssDNA, suggesting that VP2 must interact with the replicating DNA in a manner not yet identified. Replication of double-stranded MVM RF did not appear to be altered in the absence of either VP1 or VP2.

VP1 is essential for virus infectivity; however, not much is known about the infectious entry of MVM or parvoviruses in general. Ultrastructural studies have shown MVM taken up in coated pits (33), whereas canine parvovirus (CPV) appears to be taken up by endosomes and only rarely by coated vesicles (4). However, since even at a multiplicity of infection of 1, several hundred parvoviral particles are bound to the cell, it is not clear whether these uptake routes lead to a productive infection or merely lead to abortive infections. Similarly, even though virus lacking VP1 bound to cells as well as *wt* (Fig. 4), VP1 may be required to interact with a specific receptor that is necessary for virus uptake and initiation of a productive virus infection. In the human parvovirus B19, VP1 was found to be necessary to elicit neutralizing antibodies, suggesting (30) that VP1 may be found on the surface of the virus and that it interacts with a specific receptor. Alternatively, VP1 may confer a conformational change on the surface of the virion or perhaps appear only transiently on the viral surface after a partial-uncoating step, similar to the release of VP4 in picornavirus following cell binding (52).

MVM(VP1*2635*) bound cells as efficiently as *wt* at 37°C; however, in contrast to *wt* infection, in which a residual amount of the input virus (as measured by the presence of input ssDNA) remains at 12 h postinfection, none of the MVM(VP1*2635*) input ssDNA could be detected after 12 h postinfection (Fig. 5A), suggesting that the input MVM (VP1*2635*) virions might be less stable than *wt*, leaving the DNA more accessible to nucleases. These particles may become disrupted upon contact with the cells, thus leading only to an abortive infection; however, another possibility is that virions lacking VP1 are taken up normally but are unable to escape from the endosomes and are subsequently degraded. Infection by CPV is inhibited by NH_4Cl and

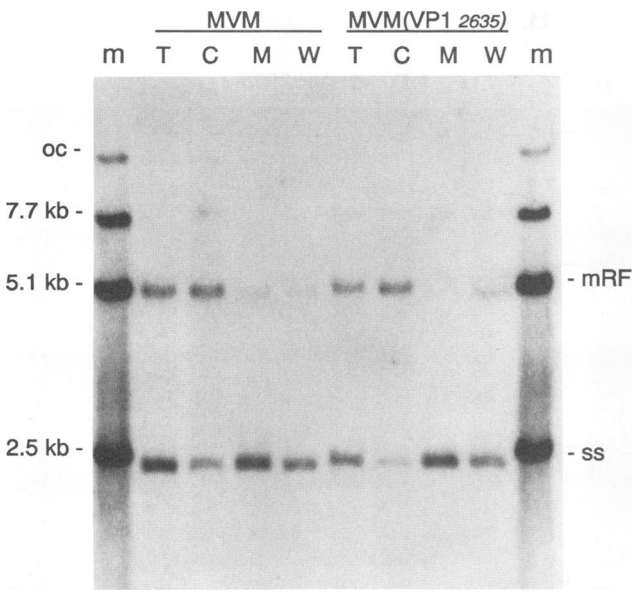

FIG. 6. Export of progeny virions to the medium 96 h after transfection with either pMVM or pMVM(VP12635). Markers (m) and viral RF are designated as described in the legend to Fig. 2. After transfection, the cells were scraped into the medium and either the total sample (T) was lysed or the cells were isolated from the medium by centrifugation, washed 3 times with an isotonic borate buffer (pH 9.0), and lysed (C). Aliquots of the cell-free medium were lysed with SDS either before (M) or after (W) the addition of the borate washes. Addition of the borate washes to the medium diluted the sample approximately twofold. Densimetric analysis of photographic negatives of ethidium bromide staining of the gel prior to Southern blotting confirmed that approximately equivalent amounts of cellular DNA had been loaded in the T and C lanes. oc, open-circular forms; ss, ssDNA.

chloroquine (4), suggesting that CPV may require exposure to an acidic environment in the lysosome for infection, and in the presence of such agents, CPV accumulates in large endosomal compartments. If MVM particles, which are also resistant to low pH (15), enter via a similar mechanism, virions lacking VP1 may be unstable at low pH and consequently degraded in the lysosome.

VP1 may also be required for the transport of MVM to the nucleus. It is not known whether MVM enters the nucleus as an intact virion or as a partially disassembled DNA-protein complex. Parvoviruses may be sufficiently small (22 nm) to pass through the nuclear pore intact; the nuclear pore can actively transport molecules of up to 25 nm in diameter (19, 21). Influenza virus RNA, on the other hand, enters the nucleus through the nuclear pore as an RNA-nucleoprotein filament (36). Several other lines of evidence also suggest that the transport of nucleic acids into the nucleus may be facilitated by karyophilic proteins. For instance, the transport of T-DNA, an approximately 20-kb ssDNA derived from the Ti plasmid of *Agrobacterium* species, into the nuclei of plant cells requires the binding of the VirE2 protein, which has two bipartite nuclear-localization signals (NLS) similar to those found in MVM VP1 as described below (12). The import of most small nuclear ribonucleoproteins into the nucleus requires the trimethylated cap as well as associated proteins (26, 40). U6 has a monomethylated cap that is not required for its nuclear localization; its transport appears to be dependent on a karyophilic U6-binding protein (40).

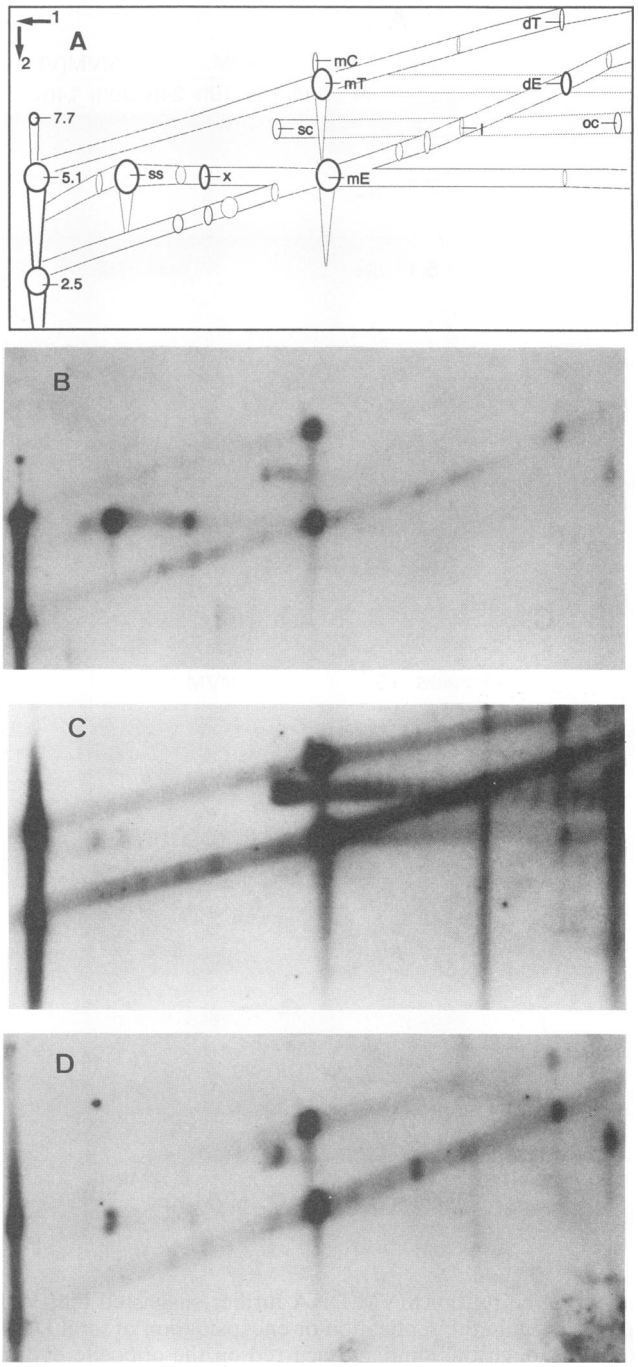

FIG. 7. MVM RF DNA separated on two-dimensional agarose gels. Shown are Southern blots of viral DNA present 60 h after transfection of $A9_{2L}$ cells with pMVM (B), pMVM(D2-A2) (C), or pMVM(D1-A1) (D). (A) Tracing of a longer exposure of the Southern blot shown in panel B. Arrows in upper-left corner of panel A show the directions of migration in the first, neutral dimension (1) and the second, alkaline (30 mM NaOH) dimension (2) for all blots. Markers, which were added at the start of the second dimension, are visible on the left. RF DNAs that have been previously characterized are designated as follows: dE, extended dimer; dT, turnaround dimer; mE, extended monomer; mT, turnaround monomer; mC, covalently closed monomer; x, band X; ss, viral ssDNA. Some input plasmid is also present (supercoiled [sc], linear [l], and nicked, open circle [oc]). A more detailed analysis of some of the previously uncharacterized DNA intermediates will be presented elsewhere (64).

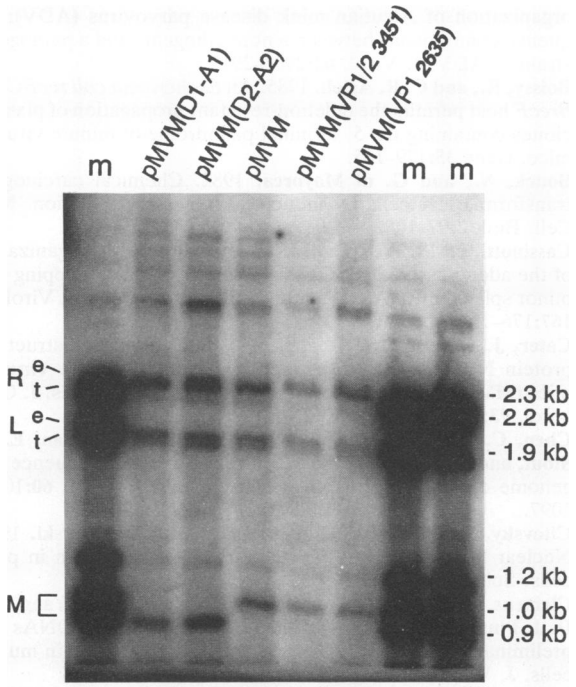

FIG. 8. Restriction enzyme analysis of viral turnaround and extended ends. Cells were lysed in 2% SDS 60 h after transfection, and low-molecular-weight DNA was isolated by a modification of the method of Hirt (28). Samples were digested with *Bst*EII (nt 1886) and *Bgl*I (nt 2872). Markers (m) were pMVM digested with *Bam*HI, *Bst*EII, and *Bgl*I. Right (R) and left (L) turnaround (t) end fragments migrate slightly faster than their extended (e) counterparts in a 1.4% agarose gel. pMVM(D1-A1) and pMVM(D2-A2) contain deletions in the middle (M) MVM fragment.

The unique, N-terminal region of VP1 is rich in basic residues, which is typical of many DNA-binding proteins, and may serve to target the incoming particle or DNA to the nuclear pore. It contains four motifs similar to those of previously described NLS (Fig. 9A). The first 10 aa (motif I) are similar to the N terminus of VP1 from simian virus 40 and polyomavirus. The first seven aa of polyomavirus VP1 have been shown by deletion analysis to be necessary and sufficient for DNA binding and may also be required for nuclear localization of that protein (41). In addition, motifs II, III, and IV contain two overlapping sequences that fit the consensus sequence for a bipartite NLS as proposed by Dingwall and Laskey (18). This signal, first characterized in nucleoplasmin, consists of two basic aa followed by a spacer of varying length and then five aa, of which at least three are basic. The minimum and maximum lengths of the spacer region have not been experimentally defined but vary between 7 and 37 aa. The large nonstructural protein of MVM, NS1, also has two sequences that fit the consensus sequence for a bipartite NLS. Mutational analysis of part of one of these sequences indicates that it may be important in the nuclear localization of that protein (45). Motifs I and IV, by virtue of having four of five basic aa, are also similar to the NLS in simian virus 40 large T antigen.

All four of these motifs are conserved among the MVM-like autonomous parvoviruses, even though the spacer regions between motifs II, III, and IV vary (Fig. 9B). PPV has an insertion between motifs III and IV; this insertion contains a K-R pair that, in conjunction with motif IV, would also fit the consensus sequence. Motifs II, III, and IV are also found in similar positions in BPV and AAV, although the N-terminal motif (I) is different. ADV VP1 appears to contain the bipartite NLS composed of motifs III and IV but

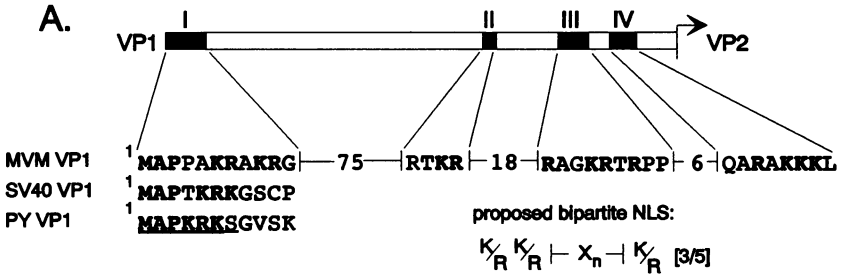

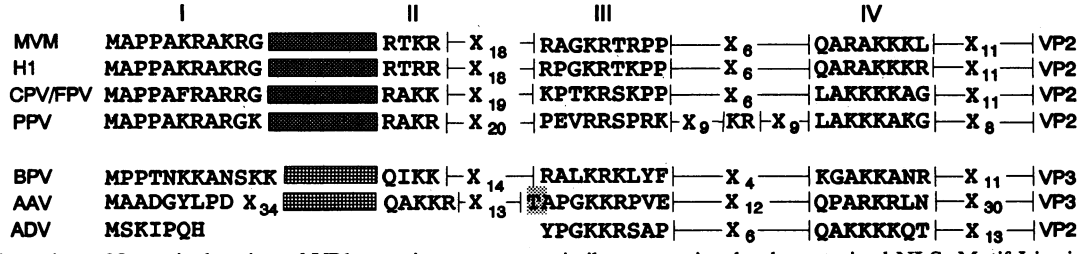

FIG. 9. The unique, N-terminal region of VP1 contains sequences similar to previously characterized NLS. Motif I is similar to the N terminus of simian virus 40 and polyomavirus VP1. Lysines and arginines within motifs II, III, and IV fit the consensus sequence for a bipartite NLS as proposed by Dingwall and Laskey (18). (B) The motifs diagrammed in panel A are conserved among the MVM-like parvoviruses (top), even though the spacer regions between motifs II, III, and IV vary. Hatched boxes represent a 75-aa region that is the most conserved domain in the parvovirus capsids and was used to align the sequences. The MVM-like parvoviruses all have approximately 75% or greater identity in this region. MVM has 65 and 55% identity in this region with BPV and AAV, respectively. AAV VP2 initiates at an ACG triplet (shaded T). Virus abbreviations and references (in parentheses): MVM (2), H1 (46, 51), CPV (47), FPV (feline parvovirus; 47), PPV (porcine parvovirus; 49), BPV (11), AAV (5, 9, 56), and ADV (1, 6).

lacks motifs I and II as well as the highly conserved domain between them that was used to align the other sequences. It has previously been proposed that the inability of ADV to spread efficiently in cell culture may be due to the lack of this sequence (1). These motifs were not found, however, in the human parvovirus B19.

Our results indicate that VP2 alone is sufficient to assemble into capsids and localize to the nucleus (data not shown), even though it does not contain a sequence similar to that of any known NLS. Therefore, if VP1 were required for the transport of the incoming particle to the nucleus, the route or mechanism of nuclear entry for the incoming particle would have to be different from that of the import of de novo-assembled empty capsids from the cytoplasm. For example, the incoming particle could bind the nuclear pore directly from the endosome and not enter the cytoplasm. Full polyomavirus virions, but not empty capsids, induce endosomes to fuse directly with the outer nuclear membrane (24).

The block to MVM mutants lacking VP1 is phenotypically similar in some respects to the block to MVM_p, the strain used in these experiments, on lymphocytes and the block to the lymphotropic strain, MVM_i, on fibroblasts. MVM_i binds to murine fibroblasts as well as MVM_p; however, it fails to initiate a productive infection (55, 57), and, like VP1 mutants, the block to MVM_i infection can be overcome by transfection (22). The primary allotropic determinant for growth in fibroblasts has been mapped to two aa within the MVM VP1- and MVM VP2-coding region and is thought to be required early during MVM infection (3). In addition, a species-specific determinant has been mapped to a similar region in CPV and feline panleukopenia virus to amino acid residues that are found on or near the viral surface (47, 61). Since these amino acids are present in both VP1 and VP2, it would be interesting to assess whether the determinant resides in VP1, in VP2, or in both. One would predict that numerous capsid mutants that are blocked at several different steps in the infectious-entry pathway of parvoviruses could be isolated. A detailed analysis of the entry of these mutants should aid in the identification of the specific steps involved early in a parvovirus infection as well as clarify the relative roles of VP1 and VP2 in infection.

ACKNOWLEDGMENTS

We thank Jerry White and the UMC Department of Plant Pathology Electron Microscope Facility for their gracious assistance and Marshall Bloom for helpful suggestions.

This work was supported by PHS grants RO1 AI21302 and KO4 AI00934 from the NIH to D.J.P.

REFERENCES

1. **Alexandersen, S., M. E. Bloom, and S. Perryman.** 1988. Detailed transcription map of Aleutian mink disease parvovirus. J. Virol. **62**:3684–3694.
2. **Astell, C. R., M. Thomson, M. Merchlinsky, and D. C. Ward.** 1983. The complete DNA sequence of minute virus of mice, an autonomous parvovirus. Nucleic Acids Res. **11**:999–1018.
3. **Ball-Goodrich, L. J., and P. Tattersall.** 1992. Two amino acid substitutions within the capsid are coordinately required for acquisition of fibrotropism by the lymphotropic strain of minute virus of mice. J. Virol. **66**:3415–3423.
4. **Basak, S., and H. Turner.** 1992. Infectious entry pathway for canine parvovirus. Virology **186**:368–376.
5. **Becerra, S. P., J. A. Rose, M. Hardy, B. M. Baroudy, and C. W. Anderson.** 1985. Direct mapping of adeno-associated virus capsid proteins B and C: a possible ACG initiation codon. Proc. Natl. Acad. Sci. USA **82**:7919–7923.
6. **Bloom, M. E., S. Alexandersen, S. Perryman, D. Lechner, and J. B. Wolfinbarger.** 1988. Nucleotide sequence and genomic organization of Aleutian mink disease parvovirus (ADV): sequence comparisons between a nonpathogenic and a pathogenic strain of ADV. J. Virol. **62**:2903–2915.
7. **Boissy, R., and C. R. Astell.** 1985. An *Escherichia coli recBC sbe BrecF* host permits the deletion-resistant propagation of plasmid clones containing the 5′ terminal palindrome of minute virus of mice. Gene **35**:179–185.
8. **Bouck, N., and G. di Mayorca.** 1982. Chemical carcinogens transform BHK cells by inducing a recessive mutation. Mol. Cell. Biol. **2**:97–105.
9. **Cassinotti, P., M. Weitz, and J.-D. Tratschin.** 1988. Organization of the adeno-associated virus (AAV) capsid gene: mapping of a minor spliced mRNA coding for virus capsid protein 1. Virology **167**:176–184.
10. **Cater, J. E., and D. J. Pintel.** 1992. The small non-structural protein NS-2 of the autonomous parvovirus minute virus of mice (MVM) is required for viral growth in murine cells. J. Gen. Virol. **73**:1839–1843.
11. **Chen, C. C., B. C. Shull, E. A. Moses, M. Lederman, E. R. Stout, and R. C. Bates.** 1986. Complete nucleotide sequence and genome organization of bovine parvovirus. J. Virol. **60**:1085–1097.
12. **Citovsky, V., J. Zupan, D. Warnick, and P. Zambryski.** 1992. Nuclear localization of *Agrobacterium* VirE2 protein in plant cells. Science **256**:1802–1805.
13. **Clemens, K. E., D. R. Cerutis, L. R. Burger, C. Q. Yang, and D. J. Pintel.** 1990. Cloning of minute virus of mice cDNAs and preliminary analysis of individual proteins expressed in murine cells. J. Virol. **64**:3967–3973.
14. **Cotmore, S. F., M. Gunther, and P. Tattersall.** 1989. Evidence for a ligation step in the DNA replication of the autonomous parvovirus minute virus of mice. J. Virol. **63**:1002–1006.
15. **Cotmore, S. F., and P. Tattersall.** 1987. The autonomously replicating parvoviruses of vertebrates. Adv. Virus Res. **33**:91–174.
16. **Cotmore, S. F., and P. Tattersall.** 1988. The NS-1 polypeptide of minute virus of mice is covalently attached to the 5′ termini of duplex replicative-form DNA and progeny single strands. J. Virol. **62**:851–860.
17. **Cotmore, S. F., and P. Tattersall.** 1989. A genome-linked copy of the NS-1 polypeptide is located on the outside of infectious parvovirus particles. J. Virol. **63**:3902–3911.
18. **Dingwall, C., and R. A. Laskey.** 1991. Nuclear targeting sequences—a consensus? Trends Biochem. Sci. **16**:478–481.
19. **Dworetzky, S. I., and C. M. Feldherr.** 1988. Translocation of RNA coated gold particles through the nuclear pore of oocytes. J. Cell Biol. **106**:575–587.
20. **Faust, E. A., and D. C. Ward.** 1979. Incomplete genomes of the parvovirus minute virus of mice: selective conservation of genome termini, including the origin for DNA replication. J. Virol. **32**:276–292.
21. **Feldherr, C. M., E. Kallenbach, and N. Schultz.** 1984. Movement of a karyophilic protein through the nuclear pores of oocytes. J. Cell Biol. **99**:2216–2222.
22. **Gardiner, E. M., and P. Tattersall.** 1988. Evidence that developmentally regulated control of gene expression by a parvoviral allotropic determinant is particle mediated. J. Virol. **62**:1713–1722.
23. **Gluzman, Y.** 1981. SV40-transformed simian cells support the replication of early SV40 mutants. Cell **23**:173.
24. **Griffith, G. R., S. J. Marriott, D. A. Rintoul, and R. A. Consigli.** 1988. Early events in polyomavirus infection: fusion of monopinocytotic vesicles containing virions with mouse kidney cell nuclei. Virus Res. **10**:41–52.
25. **Gunther, M., and B. Revet.** 1978. Study of Kilham rat virus nucleoprotein complexes extracted from infected rat cells, p. 469–477. *In* D. C. Ward and P. Tattersall (ed.), Replication of mammalian parvoviruses. Cold Spring Harbor Laboratory, Cold Spring Harbor, N.Y.
26. **Hamm, J., E. Darzynkiewicz, S. M. Tahara, and I. W. Mattaj.** 1990. The trimethylguanosine cap structure of U7 snRNA is a component of a bipartite nuclear targeting signal. Cell **62**:569–577.

27. **Hermonat, P. L., M. A. Labow, R. Wright, K. I. Berns, and N. Muzyczka.** 1984. Genetics of adeno-associated virus: isolation and preliminary characterization of adeno-associated virus type 2 mutants. J. Virol. **51**:329–339.
28. **Hirt, B.** 1967. Selective extraction of polyoma DNA from infected mouse cell cultures. J. Mol. Biol. **26**:363–369.
29. **Jongeneel, C. V., R. Sahli, G. K. McMaster, and B. Hirt.** 1986. A precise map of the splice junctions in the RNAs of the minute virus of mice, an autonomous parvovirus. J. Virol. **59**:564–573.
30. **Kajigaya, S., M. Fujii, A. Field, S. Anderson, S. Rosenfeld, L. J. Anderson, T. Shimada, and N. S. Young.** 1991. Self-assembled B19 parvovirus capsids, produced in a baculovirus system, are antigenically and immunogenically similar to native virions. Proc. Natl. Acad. Sci. USA **88**:4646–4650.
31. **Labieniec-Pintel, L., and D. Pintel.** 1986. The minute virus of mice P39 transcription unit can encode both capsid proteins. J. Virol. **57**:1163–1167.
32. **Lederman, M., D. C. Shull, E. R. Stout, and R. C. Bates.** 1987. Bovine parvovirus DNA-binding proteins: identification by a combined DNA hybridization and immunodetection assay. J. Gen. Virol. **68**:147–157.
33. **Linser, P., and R. W. Armentrout.** 1978. Binding of minute virus of mice to cells in culture, p. 151–160. *In* D. C. Ward and P. Tattersall (ed.), Replication of mammalian parvoviruses. Cold Spring Harbor Laboratory, Cold Spring Harbor, N.Y.
34. **Littlefield, J. W.** 1964. Three degrees of guanylic acid-inosine acid pyrophosphorylase deficiency in mouse fibroblasts. Nature (London) **203**:1142–1144.
35. **Maniatis, T., E. F. Fritsch, and J. Sambrook.** 1982. Molecular cloning: a laboratory manual, p. 473. Cold Spring Harbor Laboratory, Cold Spring Harbor, N.Y.
36. **Martin, K., and A. Helenius.** 1991. Transport of incoming influenza virus nucleocapsids into the nucleus. J. Virol. **65**:232–244.
37. **Merchlinsky, M. J.** 1984. Studies on MVM DNA replication using an infectious molecular clone. Ph.D. thesis. Yale University, New Haven, Conn.
38. **Merchlinsky, M. J., P. J. Tattersall, J. J. Leary, S. F. Cotmore, E. M. Gardiner, and D. C. Ward.** 1983. Construction of an infectious molecular clone of the autonomous parvovirus minute virus of mice. J. Virol. **47**:227–232.
39. **Metcalf, J. B., R. C. Bates, and M. Lederman.** 1990. Interaction of virally coded protein and a cell cycle-regulated cellular protein with the bovine parvovirus left terminus *ori*. J. Virol. **64**:5485–5490.
40. **Michaud, N., and D. S. Goldfarb.** 1991. Multiple pathways in nuclear transport: the import of U2 snRNP occurs by a novel kinetic pathway. J. Cell Biol. **112**:215–223.
41. **Moreland, R. B., L. Montross, and R. L. Garcea.** 1991. Characterization of the DNA-binding properties of the polyomavirus capsid protein VP1. J. Virol. **65**:1168–1176.
42. **Morgan, W. R., and D. C. Ward.** 1986. Three splicing patterns are used to excise the small intron common to all minute virus of mice RNAs. J. Virol. **60**:1170–1174.
43. **Naeger, L. K., J. Cater, and D. J. Pintel.** 1990. The small nonstructural protein (NS2) of the parvovirus minute virus of mice is required for efficient DNA replication and infectious virus production in a cell-type-specific manner. J. Virol. **64**: 6166–6175.
44. **Naeger, L. K., N. Salome, and D. J. Pintel.** Submitted for publication.
45. **Nuesch, J. P. F., and P. Tattersall.** 1992. Personal communication.
46. **Paradiso, P. R., K. R. Williams, and R. L. Costantino.** 1984. Mapping of the amino terminus of the H-1 parvovirus major capsid protein. J. Virol. **52**:77–81.
47. **Parrish, C. R., C. F. Aquadro, and L. E. Carmichael.** 1988. Canine host range and a specific epitope map along with variant sequences in the capsid protein gene of canine parvovirus and related feline, mink, and raccoon. Virology **166**:293–307.
48. **Peterson, J. L., K. Dale, R. Karess, D. Leonard, and D. C. Ward.** 1978. Comparison of parvovirus structural proteins: evidence for post-translational modification, p. 431–445. *In* D. C. Ward and P. Tattersall (ed.), Replication of mammalian parvoviruses. Cold Spring Harbor Laboratory, Cold Spring Harbor, N.Y.
49. **Ranz, A. I., J. J. Manclús, E. Díaz-Aroca, and J. I. Casal.** 1989. Porcine parvovirus: DNA sequence and genome organization. J. Gen. Virol. **70**:2541–2553.
50. **Rhode, S. L., III.** 1976. Replication process of the parvovirus H-1. V. Isolation and characterization of temperature-sensitive H-1 mutants defective in progeny DNA synthesis. J. Virol. **17**:659–667.
51. **Rhode, S. L., III, and P. R. Paradiso.** 1983. Parvovirus genome: nucleotide sequence of H-1 and mapping of its genes by hybrid-arrested translation. J. Virol. **45**:173–184.
52. **Rueckert, R. R.** 1991. Picornaviridae and their replication, p. 409–450. *In* B. N. Fields, D. M. Knipe et al. (ed.), Fundamental virology, 2nd ed. Raven Press, Ltd., New York.
53. **Schoborg, R. V., Q. Zhao, and D. J. Pintel.** Unpublished data.
54. **Southern, E. M.** 1975. Detection of specific sequences among DNA fragments separated by gel electrophoresis. J. Mol. Biol. **98**:503–517.
55. **Spalholz, B. A., and P. Tattersall.** 1983. Interaction of minute virus of mice with differentiated cells: strain-dependent target cell specificity is mediated by intracellular factors. J. Virol. **46**:937–943.
56. **Srivastava, A., E. W. Lusby, and K. I. Berns.** 1983. Nucleotide sequence and organization of the adeno-associated virus 2 genome. J. Virol. **45**:555–564.
57. **Tattersall, P., and J. Bratton.** 1983. Reciprocal productive and restrictive virus-cell interactions of immunosuppressive and prototype strains of minute virus of mice. J. Virol. **46**:944–955.
58. **Tattersall, P., P. J. Cawte, A. J. Shatkin, and D. C. Ward.** 1976. Three structural polypeptides coded for by minute virus of mice, a parvovirus. J. Virol. **20**:273–289.
59. **Tattersall, P., A. J. Shatkin, and D. C. Ward.** 1977. Sequence homology between the structural polypeptides of minute virus of mice. J. Mol. Biol. **111**:375–394.
60. **Tratschin, J. D., I. L. Miller, and B. J. Carter.** 1984. Genetic analysis of adeno-associated virus: properties of deletion mutants constructed in vitro and evidence for an adeno-associated virus replication function. J. Virol. **51**:611–619.
61. **Tsao, J., M. S. Chapman, M. Agbandje, W. Keller, K. Smith, H. Wu, M. Luo, T. J. Smith, M. G. Rossmann, R. W. Compans, and C. R. Parrish.** 1991. The three-dimensional structure of canine parvovirus and its functional implications. Science **251**:1456–1464.

61a. **Tullis, G. E.** Unpublished results.

62. **Tullis, G. E., L. R. Burger, and D. J. Pintel.** Virology, in press.
63. **Tullis, G. E., L. Labieniec-Pintel, K. E. Clemens, and D. Pintel.** 1988. Generation and characterization of a temperature-sensitive mutation in the NS-1 gene of the autonomous parvovirus minute virus of mice. J. Virol. **62**:2736–2744.
64. **Tullis, G. E., R. V. Schoborg, and D. J. Pintel.** Unpublished data.
65. **Willwand, K., and B. Hirt.** 1991. The minute virus of mice capsid specifically recognizes the 3′ hairpin structure of the viral replicative-form DNA: mapping of the binding site by hydroxyl radical footprinting. J. Virol. **65**:4629–4635.
66. **Willwand, K., and O.-R. Kaaden.** 1990. Proteins of viral and cellular origin bind to the Aleutian disease virus (ADV) DNA 3′ terminal hairpin: presentation of a scheme for encapsidation of ADV DNA. J. Virol. **64**:1598–1605.
67. **Yakobson, B., T. A. Hrynko, M. J. Peak, and E. Winocour.** 1989. Replication of adeno-associated virus in cells irradiated with UV light at 254 nm. J. Virol. **63**:1023–1030.